**Zero : Jurnal Sains, Matematika, dan Terapan**
E-ISSN : 2580-5754; P-ISSN : 2580-569X
Volume 9, Number 3, 2025
DOI: 10.30829/zero.v9i3.25692
Page: 752 - 765

# Modeling Monthly Rainfall Data Using the Alpha Power Transformed X-Lindley Distribution in the Toba Lake Region

[1] **Mohamad Khoirun Najib**
Division of Computational Mathematics, IPB University, Indonesia

[2] **Sri Nurdiati**
Division of Computational Mathematics, IPB University, Indonesia

[3] **Elis Khatizah**
Division of Computational Mathematics, IPB University, Indonesia

[4] **Aulia Rizki Firdawanti**
Division of Statistical Modelling and Data Analysi, IPB University, Indonesia

[5] **Hendri Irwandi**
Research Center for Climate and Atmosphere, National Research and Innovation Agency, Indonesia

[6] **Mirza Farhan Azhari**
Master's Student of Applied Mathematics, IPB University, Indonesia

[7] **David Vijanarco Martal**
Master's Student of Applied Mathematics, IPB University, Indonesia

[8] **Nicholas Abisha**
Master's Student of Applied Mathematics, IPB University, Indonesia

**Article Info**

*Article history:*

Accepted 26 December 2025

*Keywords:*

Alpha Power Transformation;
Goodness-of-Fit Criteria;
Maximum Likelihood Estimation;
Probabilistic Rainfall Modeling;
X-Lindley Distribution.

**ABSTRACT**

Modeling rainfall is crucial for hydrological studies and climate adaptation, especially in regions with complex topography such as the Toba Lake area, North Sumatra. Classical probability distributions often struggle to represent skewness, heavy tails, and variability observed in tropical rainfall. This study explores APTXL distribution as a flexible two-parameter model. Through the alpha power transformation, APTXL extends the X-Lindley distribution by introducing an additional shape parameter, allowing better accommodation of asymmetrical and extreme values while maintaining analytical tractability. Statistical properties are derived, and parameters are estimated using maximum likelihood. The model is applied to a long-term dataset from 13 meteorological stations, covering 408 monthly observations per station. Comparative analysis against Gamma, Lognormal, and Generalized Extreme Value distributions using multiple goodness-of-fit criteria indicates that APTXL provides consistently improved performance. These results suggest APTXL as a practical tool for rainfall modeling and water-resource applications in climate-sensitive regions.

*Corresponding Author:*

Mohamad Khoirun Najib,
Division of Computational Mathematics, School of Data Science, Mathematics, and Informatics,
IPB University, Bogor, Indonesia
Email: mkhoirun@apps.ipb.ac.id

## 1. INTRODUCTION

Rainfall is a fundamental component of the Earth's climate system, playing a pivotal role in hydrological processes [1], [2], water resource sustainability [3], agricultural productivity [4], urban planning [5], and disaster risk mitigation [6]. In tropical countries such as Indonesia, rainfall exhibits high spatiotemporal variability and frequent extreme events [7], [8], which introduce significant uncertainty into water management and climate adaptation planning. This variability complicates the prediction of hydrological responses and increases the risk of floods, landslides, and droughts [9], [10], especially in ecologically sensitive and economically vital regions such as the Toba Lake area in North Sumatra.

The Toba Lake region is characterized by a complex hydrometeorological setting influenced by volcanic topography, steep elevation gradients, and a large caldera lake that affects local weather dynamics [11], [12]. Monthly rainfall in this area shows substantial temporal fluctuation and spatial heterogeneity [13], often with high positive skewness and heavy-tailed distributions. These statistical characteristics present significant challenges for traditional probabilistic models, which generally rely on assumptions of symmetry and light-tailed behavior.

Rainfall modeling is not only of academic interest but also directly informs practical decision-making systems, including reservoir operation planning [14], agricultural scheduling [15], [16], and hydrometeorological early warning systems [17], [18]. Accurate representation of extremes is essential for managing flood risk [19], [20], while reliable estimates of central tendencies support water allocation and long-term resource planning [21], [22]. Classical probability distributions such as the Gamma [23], Lognormal [24], and Generalized Extreme Value [25] have been widely employed in modeling rainfall data due to their mathematical simplicity and analytical convenience. However, their ability to capture the full complexity of empirical rainfall distributions is often limited [26], particularly in tropical regions where extremes and distributional asymmetry are common. To overcome these shortcomings, more flexible approaches like mixture distributions [27], [28] and copula-based models [29], [30] have been explored, offering improved fit at the expense of substantially higher computational demands. These limitations underscore the need for more flexible probability models that can provide a better fit to observed data and enhance statistical inference.

To address this gap, the present study investigates the Alpha Power Transformed X-Lindley (APTXL) distribution [31], a two-parameter model derived from the X-Lindley distribution through an alpha power transformation. Through this transformation, an additional shape parameter is introduced, enabling the model to accommodate a broader range of skewness and kurtosis. Unlike the Alpha Power Transformed Lindley (APT–Lindley) distribution [32], which modifies the standard Lindley baseline, APTXL is constructed from the X-Lindley distribution, thereby offering distinct flexibility in handling heavier tails and asymmetry while still maintaining analytical tractability. This distinction is important because the X-Lindley baseline itself has different tail properties compared to the Lindley distribution, which makes the transformed version (APTXL) better suited for highly variable rainfall data.

This study presents an analytical investigation of the statistical properties of the APTXL distribution, including its probability density function, cumulative distribution function, and quantile function. Moreover, the estimation performance of the model parameters using Maximum Likelihood Estimation (MLE) is evaluated through simulation experiments under varying sample sizes. The practical motivation for applying APTXL arises from evidence that classical distributions such as Gamma, Lognormal, and Generalized Extreme Value often underestimate rainfall extremes and fail to capture heavy skewness in tropical climates [23], [24], [26]. Such shortcomings have been documented in various studies of Indonesia and other tropical regions, where rainfall exhibits marked asymmetry and frequent extreme values [9], [10]. To evaluate its effectiveness in this context, this study applies the APTXL model to long-term monthly rainfall data from the Toba Lake region and compares its performance with Gamma, Lognormal, and GEV distributions using multiple goodness-of-fit metrics (AIC, RMSE, KS, and CM).

Recent advances in alpha-power–type transformations have considerably broadened the Lindley/X-Lindley family for environmental applications. Beyond the classical Lindley distribution, newer variants such as the alpha power transformation of the Lindley distribution (APTLD) formalize a multi-parameter generalization with richer tail behavior and flexible hazards, demonstrating improved fits on skewed data sets [33]. Related extensions include the alpha power–transformed extended power Lindley (APTEPL) model, which shows tangible gains over earlier Lindley-type baselines [34]. Within the X-Lindley lineage, 2024 developments such as the power new X-Lindley distribution likewise reinforce the utility of power-transformation strategies to control skewness and kurtosis with minimal parameter overhead [35]. These advances align with our choice to employ an alpha-power transformation over the X-Lindley baseline for tropical rainfall, where right-tail realism is essential.

Parallel progress has occurred in stochastic rainfall modelling. A contemporary review synthesizes temporal and space–time point-process formulations and fitting strategies, underscoring the role of mechanistic structure when representing extremes [36]. New generators—e.g., STORM v.2—enable controlled exploration of climate-change impacts at hydrologically relevant scales [37], and serial-type stochastic rainfall generators emphasize unprecedented events in daily sequences, improving design-oriented hydrological analysis [38]. Complementing generators, comparative distributional studies continue to benchmark candidates for extremes; a 1972–2022 assessment shows when log-Gumbel or three-parameter log-normal outperform competitors for different return-period ranges, illustrating why flexible, tail-aware models remain necessary [39]. Within the X-Lindley sphere itself, an XLindley extension with rainfall application further validates the practical relevance of this baseline for precipitation data [31].

From a hydrological applications and optimal design perspective, recent international works emphasize decision support under data and network constraints. Large-scale rain-gauge network optimization workflows have been proposed to balance computational tractability with coverage of heterogeneous terrains [40], while entropy–copula frameworks and MADM-style approaches provide rank-based criteria for network design and prioritization in operational contexts [41]. On the analysis side, updated IDF-curve derivations informed by distributional testing enhance flood-risk diagnostics in rapidly urbanizing regions [42]. Collectively, these contributions motivate rainfall models that are (i) parsimonious yet tail-responsive, (ii) compatible with stochastic generators and design studies, and (iii) robust across stations with varying hydro-climatic regimes—criteria satisfied by the APTXL formulation evaluated here.

## 2. RESEARCH METHOD

The methodological framework of this study is structured to present both the theoretical formulation of the proposed model and its empirical application to rainfall data. The section begins with a detailed exposition of the Alpha Power Transformed X-Lindley (APTXL) distribution, including its probability functions and key statistical properties. Following this, the procedures for parameter estimation are outlined, with emphasis on the maximum likelihood approach and the numerical optimization routine used. Goodness-of-fit evaluation criteria are then introduced to assess the adequacy of the APTXL distribution in comparison with classical alternatives such as the Gamma, Lognormal, and Generalized Extreme Value models. Finally, simulation experiments and empirical applications are described to validate the consistency of the estimation method and to demonstrate the practical relevance of the distribution for hydrological data.

### 2.1. Alpha Power Transformed X-Lindley (APTXL) Distribution

Mahdavi and Kundu [43] introduced a family of lifetime distributions known as the Alpha Power Transformation (APT) method, which generalizes a baseline distribution by incorporating an additional shape parameter. Since its introduction, the APT method has been widely adopted by researchers to develop more flexible probabilistic models. For instance, Nassar et al. [44] proposed the alpha power Weibull distribution, Basheer [45] introduced the alpha power inverse Weibull distribution, Dey et al. [32] suggested the alpha power transformed Lindley distribution, and in a separate study, Dey et al. [46] developed the alpha power transformed inverse Lindley distribution. Furthermore, Ihtisham et al. [47] explored the alpha power Pareto distribution, while Zeineldin et al. [48] proposed the alpha power inverse Lomax distribution.

The Alpha Power Transformed X-Lindley (APTXL) distribution [31] is a two-parameter probability model developed to enhance the modeling flexibility of the original X-Lindley distribution [49]. Introduced as part of the alpha power transformation family, this model incorporates an additional shape parameter that regulates the tail behavior and asymmetry of the distribution. Such a transformation enables the APTXL to represent a wider variety of empirical data patterns, particularly those exhibiting positive skewness and heavy tails, characteristics commonly observed in environmental and hydrological variables.

**Definition 1.** Let $X$ be a random variable following the alpha power transformed X-Lindley distribution with parameter $\alpha > 0$ and $\theta > 0$. Its probability density function (pdf) is given by:

$$f(x;\alpha,\theta) = \begin{cases} \dfrac{\ln(\alpha)}{\alpha-1}\alpha^{\left[1-\left(1+\frac{\theta x}{(1+\theta)^2}\right)e^{-\theta x}\right]}\dfrac{\theta^2(2+\theta+x)e^{-\theta x}}{(1+\theta)^2}, & \text{if } \alpha \neq 1 \\ \dfrac{\theta^2(2+\theta+x)e^{-\theta x}}{(1+\theta)^2}, & \text{if } \alpha = 1 \end{cases} \tag{1}$$

and the corresponding cumulative distribution function (cdf) is:

$$F(x;,\alpha,\theta)=\begin{cases}\dfrac{\alpha^{\left[1-\left(1+\frac{\theta x}{(1+\theta)^2}\right)e^{-\theta x}\right]}-1}{\alpha-1}, & \text{if } \alpha\neq 1\\ 1-\left(1+\dfrac{\theta x}{(1+\theta)^2}\right)e^{-\theta x}, & \text{if } \alpha=1\end{cases} \tag{2}$$

The random variable $X$ has support $x\in(0,\infty)$, governed by shape parameter $\alpha>0$ and scale parameter $\theta>0$. When $\alpha=1$, the distribution reduces to the original X-Lindley model. The additional parameter $\alpha$ gives APTXL great flexibility: for $\alpha>1$, the pdf becomes more right-skewed and heavy-tailed, and for $0<\alpha<1$, the pdf shifts mass to the left, producing lighter upper tails.

The quantile function $Q(u)=F^{-1}(u), 0<u<1$, is required in stochastic simulation and statistical applications, and is given by:

$$Q(u;\alpha,\theta)=-\frac{(1+\theta)^2}{\theta}-\frac{1}{\theta}W_{-1}\left[\frac{e^{-(1+\theta)^2}(1+\theta)^2\big(\ln\big(1+u(-1+\alpha)\big)-\ln(\alpha)\big)-\ln(\alpha)}{\ln(\alpha)}\right] \tag{3}$$

Using the quantile function, the random variable $X=Q(V;\alpha,\theta)$ has density function (Eq. 1), where $V$ is a uniform random variable over the interval (0, 1).

These properties demonstrate that the APTXL distribution provides a flexible yet analytically tractable framework for modeling skewed and heavy-tailed data. Its ability to adjust both scale and tail behavior through the parameters $\theta$and $\alpha$makes it particularly suitable for hydrological applications where extremes are of central concern. Having established the theoretical basis of the model, the next step is to discuss the estimation of its parameters and the procedures used to assess its empirical adequacy.

### 2.2. Parameter Estimation

Let the random variables $X_1,X_2,\dots,X_n\sim APTXL(\alpha,\theta)$ with observed values $x_1,x_2,..,x_n$. From (Eq.1), the log-likelihood function can be written as

$$\begin{aligned}l(\alpha,\theta;x)&=\ln\prod_{i=1}^{n}f(x_i;\alpha,\theta)\\&=\sum_{i=1}^{n}\ln\left(\frac{\ln(\alpha)}{\alpha-1}\alpha^{\left[1-\left(1+\frac{\theta x}{(1+\theta)^2}\right)e^{-\theta x}\right]}\frac{\theta^2(2+\theta+x)e^{-\theta x}}{(1+\theta)^2}\right)\\&=\sum_{i=1}^{n}\ln\left(\frac{\ln(\alpha)}{\alpha-1}\right)+\sum_{i=1}^{n}\left[1-\left(1+\frac{\theta x}{(1+\theta)^2}\right)e^{-\theta x}\right]\ln\alpha+\sum_{i=1}^{n}\ln\left(\frac{\theta^2(2+\theta+x)e^{-\theta x}}{(1+\theta)^2}\right)\\&=n\ln(\ln(\alpha))-n\ln(\alpha-1)+\ln(\alpha)\sum_{i=1}^{n}\left(1-\left(1+\frac{\theta x_i}{(1+\theta)^2}\right)e_i^{-\theta x_i}\right)+2n\ln(\theta)\\&\quad+\sum_{i=1}^{n}\ln(2+\theta+x_i)-\theta\sum_{i=1}^{n}x_i-2n\ln(1+\theta)\end{aligned} \tag{4}$$

To estimate the maximum likelihood values of parameters α and θ, Equation 4 can be directly maximized with respect to both parameters. Since the function is nonlinear, the maximum value of the log-likelihood can be determined using numerical optimization methods. One such method is the Nelder-Mead simplex algorithm [50]. The task of maximizing the likelihood is reformulated as minimizing the negative log-likelihood function, making the objective function to be minimized as:

$$\alpha,\theta=\min_{\alpha,\theta}-l(\alpha,\theta) \tag{5}$$

To estimate the parameters $\alpha$ and $\theta$, the negative log-likelihood function (Eq. 5) was minimized using the Nelder–Mead simplex algorithm, a derivative-free optimization routine widely applied in likelihood-based estimation. The algorithm iteratively updates a simplex of candidate solutions through reflection, expansion, contraction, and shrinkage operations until convergence. Convergence was declared when successive iterations satisfied both (i) a relative change in the objective function below $10^{-8}$ and (ii) a relative change in parameter values below $10^{-6}$, or when the maximum number of iterations (10,000) was reached. To avoid local optima, the optimization was initialized with multiple starting values obtained from method-of-moments estimates and from uniform random draws within plausible parameter ranges ($\alpha,\theta>0$). In practice, stable convergence was consistently achieved across all stations, and the final solutions were insensitive to the choice of initial values.

### 2.3. Goodness-of-Fits Test

To evaluate whether the APTXL distribution provides an adequate representation of monthly rainfall data, a set of complementary goodness-of-fit criteria was applied. The Akaike Information Criterion (AIC) was used to balance model parsimony and quality of fit, defined as

$$AIC = 2k - 2\ln L, \tag{6}$$

where $k$ denotes the number of estimated parameters and $L$ is the maximized likelihood function. The Root Mean Square Error (RMSE) was considered to measure the magnitude of predictive errors, expressed as

$$RMSE = \sqrt{\frac{1}{n}\sum_{i=1}^{n}(P_{Ei} - P_{Ti})^2}, \tag{7}$$

with $n$ denoting the sample size, $P_{Ei}$ the empirical frequencies, and $P_{Ti}$ the theoretical frequencies. The Kolmogorov–Smirnov (KS) statistic was employed to capture the maximum absolute difference between the empirical and theoretical distributions, given by

$$KS = \max_{i=1,2,\ldots,n} |P_{Ei} - P_{Ti}|. \tag{8}$$

Finally, the Cramér–von Mises (CM) statistic was used to assess overall discrepancies between the empirical and fitted cumulative distribution functions, computed as

$$T = \frac{1}{12n} + \sum_{i=1}^{n}\left[\frac{2i-1}{2n} - F(x_i)\right]^2 \tag{9}$$

where $F(x_i)$ is the theoretical cumulative distribution evaluated at the ordered sample values $x_i$. Together, these metrics provide a comprehensive assessment of model adequacy, since each emphasizes a distinct dimension of fit quality, from parsimony and error magnitude to local and global distributional differences.

To perform a comprehensive and objective comparison across all 13 rainfall stations and multiple statistical criteria, this study adopts the *Comprehensive Rating Index* (CRI) [51], [52]. The CRI is a normalized index that aggregates the ranks of each distribution across all stations and all metrics:

$$CRI_j = 1 - \frac{1}{S \times M \times N}\sum_{i=1}^{S}\sum_{k=1}^{M} Rank_{ijk} \tag{10}$$

where $CRI_j$ is comprehensive rating index for distribution $j$, $Rank_{ijk}$ is rank of distribution $j$ at station $i$ under metric $k$ (1 = best to 4 = worst), $S$ is number of stations (13), $M$ is number of evaluation metrics (4), and $N$ is number of candidate distributions (4: APTXL, Gamma, Lognormal, GEV).

The decision to employ aggregated ranks rather than direct normalization offers clear methodological advantages for evaluating competing distributions. By converting raw values of AIC, RMSE, KS, and CM into ranks, differences in measurement scales and units are eliminated, which allows each criterion to contribute equally to the overall assessment. This approach ensures that a metric expressed in large absolute numbers, such as AIC, does not overshadow another metric like KS or CM, which typically yields smaller values. Moreover, rank aggregation provides a more robust summary by reducing the undue influence of extreme values. For instance, if one distribution produces an unusually high RMSE at a single station, normalization of raw scores would heavily penalize that model across the entire evaluation. In contrast, when using ranks, the impact of this anomaly is limited to one criterion at one station, preserving the fairness of the overall index. The Comprehensive Rating Index (CRI) derived from aggregated ranks therefore captures the consistency of model performance across stations and metrics, rather than being driven by isolated outliers. In hydrological applications, where rainfall distributions can vary widely across space and time, such stability is particularly valuable because it reflects general reliability rather than sensitivity to extreme local fluctuations.

## 3. RESULTS AND DISCUSSION

### 3.1. Simulation

To evaluate the accuracy of the estimation method, we employ a Monte Carlo simulation approach with 10,000 replications, adopted from [53]. Three scenarios are considered, using sample sizes n = {50, 100, 500}. Random samples are generated based on Eq. 3, with true parameter values set to $\alpha = 0.5$ and $\theta = 0.5$ for Scenario 1, $\alpha = 0.5$ and $b = 1$ for Scenario 2, and $\alpha = 1.5$ and $b = 1.5$ for Scenario 3. They provide a controlled variation in both shape ($\alpha$) and scale ($\theta$) that allows assessment of estimation performance across light-tailed, moderate, and heavy-tailed conditions. Thus, while simplified, the scenarios approximate realistic rainfall characteristics,

enabling the simulation study to be both interpretable and relevant to the empirical application. Table 1 presents the simulation results across all scenarios, including the average estimator (AE) over 10,000 replications, the bias of AE relative to the true parameter values, and the mean squared error (MSE) for each sample. As expected, the MLE estimates converge to the true values, and both bias and MSE decrease as the sample size n increases.

**Table 1.** Simulation results (Average estimator AE, Absolute bias AB, and MSE) for different sample sizes $n$ and scenarios.

| $n$ | Parameters | Estimation | Scenario 1 ($\alpha = 0.5, \theta = 0.5$) | Scenario 2 ($\alpha = 0.5, \theta = 1$) | Scenario 3 ($\alpha = 1.5, \theta = 1.5$) |
|---|---|---|---|---|---|
| 50 | α | AE | 1.1117 | 1.0767 | 2.6100 |
| | | AB | 0.6117 | 0.5767 | 1.1100 |
| | | MSE | 2.8719 | 17.002 | 11.030 |
| | θ | AE | 0.5289 | 1.0597 | 1.5521 |
| | | AB | 0.0289 | 0.0597 | 0.0521 |
| | | MSE | 0.0240 | 0.1069 | 0.1355 |
| 100 | α | AE | 0.7728 | 0.7674 | 1.9646 |
| | | AB | 0.2728 | 0.2674 | 0.4646 |
| | | MSE | 0.6334 | 15.005 | 2.2450 |
| | θ | AE | 0.5078 | 1.0149 | 1.5269 |
| | | AB | 0.0078 | 0.0149 | 0.0269 |
| | | MSE | 0.0147 | 0.0609 | 0.0603 |
| 500 | α | AE | 0.5440 | 0.5401 | 1.5835 |
| | | AB | 0.0440 | 0.0401 | 0.0835 |
| | | MSE | 0.0638 | 0.0516 | 0.2472 |
| | θ | AE | 0.5001 | 1.0012 | 1.5045 |
| | | AB | 0.0001 | 0.0012 | 0.0045 |
| | | MSE | 0.0030 | 0.0121 | 0.0111 |

Table 1 summarizes the results of a Monte Carlo simulation study designed to assess the performance of the maximum likelihood estimation (MLE) method for the APTXL distribution under three different parameter settings and varying sample sizes. For each scenario, the table reports the average estimator (AE), absolute bias (AB), and mean squared error (MSE) based on 10,000 simulated samples of size $n$ = 50, 100, and 500. The simulation results confirm that the maximum likelihood estimators for both parameters of the APTXL distribution are consistent and asymptotically unbiased. Both the absolute bias and MSE decrease systematically with increasing sample size, validating the reliability of the proposed estimation method in practical applications. The results also highlight that while estimation of $\alpha$ can be more sensitive to sample size, particularly in heavy-tailed settings, the estimation of $\theta$ remains comparatively stable and efficient. To aid interpretation, we complement Table 1 with line plots of AE and MSE against sample size $n$ for $\alpha$ and $\theta$ across the three scenarios. Figure 1 highlight the expected consistency of MLE (AE approaching the true parameters) and efficiency gains (MSE decreasing with $n$).

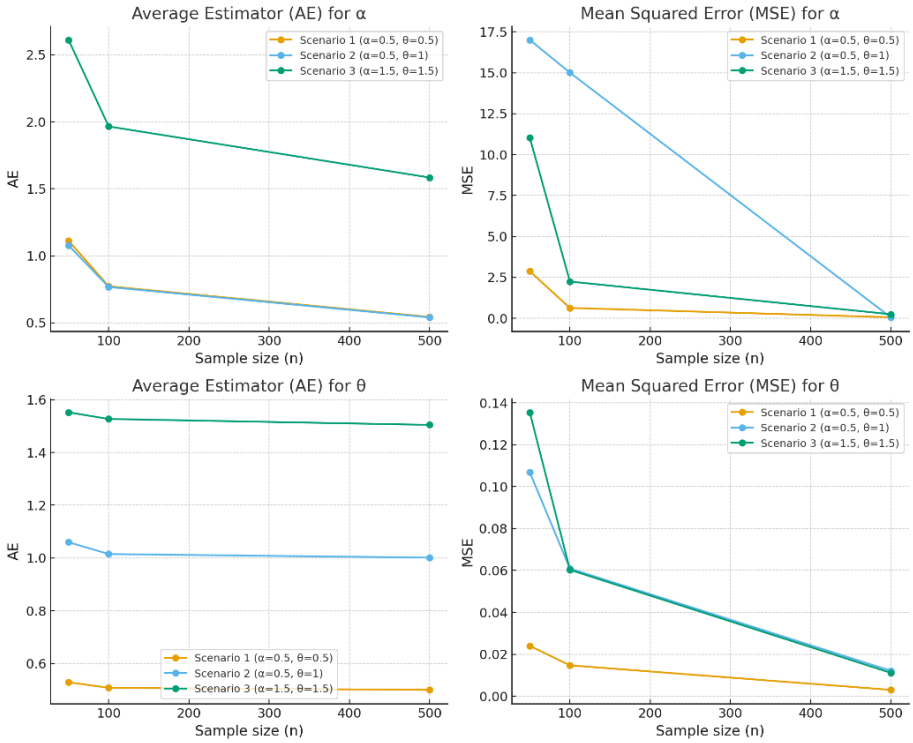


Figure 1. Monte Carlo simulation results showing AE and MSE for $\alpha$ and $\theta$ across three scenarios, illustrating convergence of MLE estimates to true parameters and decreasing MSE with larger sample sizes.

Figure 1 provides a visual validation of the theoretical properties of the MLE for APTXL parameters. In all scenarios, the AE curves for both $\alpha$ and $\theta$ move closer to the true parameter values as the sample size grows, indicating unbiasedness in large samples. Simultaneously, the MSE curves decline sharply with increasing nnn, showing efficiency gains and reduced estimation variability. Notably, scenarios with heavier tails (e.g., $\alpha = 1.5, \theta = 1.5$) exhibit larger deviations at smaller sample sizes, but these stabilize rapidly as $n$ increases. Overall, the figure illustrates that MLE remains reliable for both shape and scale parameters of the APTXL distribution, with performance improving markedly as the amount of data grows.

In practical terms, the simulation results highlight how the two parameters of the APTXL distribution, $\alpha$and $\theta$, govern different aspects of rainfall behavior. The parameter $\alpha$primarily controls the heaviness of the distribution's tail and thus reflects the probability of observing extreme rainfall events. Larger values of $\alpha$generate heavier right tails, implying an increased likelihood of unusually high rainfall totals, while smaller values of $\alpha$shift the mass toward the body of the distribution, reducing the probability of extremes. This interpretation is particularly important in hydrological applications, since tail behavior directly affects flood risk assessment and early warning systems. The parameter $\theta$, on the other hand, acts as a scale factor that determines the overall spread of rainfall values. Higher values of $\theta$correspond to broader variability and larger expected totals, whereas lower values compress the distribution, producing lower mean rainfall. When considered jointly, $\alpha$and $\theta$provide a flexible way of characterizing both the typical monthly rainfall levels and the likelihood of extreme events. The simulation confirms that their maximum likelihood estimates converge toward the true values as sample size increases, reinforcing the reliability of these parameters as interpretable indicators of rainfall intensity and variability.

### 3.2. Application to Monthly Rainfall Data

To demonstrate the practical applicability of the APTXL distribution, this section presents an empirical analysis of long-term monthly rainfall data from the Toba Lake region in North Sumatra, Indonesia. The objective is to evaluate the goodness-of-fit performance of the proposed model in capturing the distributional characteristics of real-world hydrological data, particularly in a tropical setting with known variability and extremes. The region is well suited for this purpose, as its complex topography and climatic conditions produce highly skewed and heavy-tailed rainfall patterns. By comparing APTXL with classical models, the analysis assesses not only its ability to describe average behavior but also its effectiveness in representing extreme rainfall events that are critical for hydrological risk management.

### 3.2.1. Dataset

This study utilizes a comprehensive monthly rainfall dataset from 13 meteorological observation stations located in the Toba Lake region, North Sumatra, Indonesia. The dataset spans a 34-year period, from January 1981 to December 2014, resulting in 408 monthly observations per station. Each station record includes metadata such as station name, geographical coordinates (latitude and longitude), and a continuous time series of monthly rainfall totals (in millimeters). The selection of the Toba Lake region is motivated by its complex topography and hydrometeorological importance. The area features a large volcanic caldera lake surrounded by steep highlands, which significantly influence local precipitation patterns. Consequently, rainfall in this region tends to exhibit high temporal variability, spatial heterogeneity, and extreme values, conditions that challenge standard statistical models and motivate the use of more flexible probability distributions such as the APTXL. The 13 observation stations used in this analysis include: Dolok Sanggul, Merek, Onanrunggu, Pangururan, Stage of Parapat, Siborongborong, Laguboti, Lumban Julu, Silaen, Sidamanik, Parlilitan, Sitinjo, and Gabe Hutaraja.

**Table 2.** Simplified descriptive statistics of monthly rainfall (in mm) per station (1981–2014).

| Station | Mean | Std. | Min. | Median | Max. | Skewness | Excess Kurtosis |
|---|---|---|---|---|---|---|---|
| Dolok Sanggul | 176.05 | 105.77 | 3 | 163 | 715 | 0.78 | 1.13 |
| Merek | 182.44 | 111.74 | 8 | 163 | 916 | 1.74 | 6.66 |
| Onanrunggu | 161.67 | 96.30 | 7 | 152 | 490 | 0.74 | 0.32 |
| Pangururan | 155.90 | 90.79 | 0 | 145 | 542 | 0.78 | 0.67 |
| Stageof Parapat | 175.34 | 95.73 | 2 | 164 | 577 | 0.73 | 0.65 |
| Siborong-borong | 181.07 | 111.15 | 2 | 164 | 548 | 0.72 | 0.22 |
| Laguboti | 145.97 | 88.64 | 2 | 133 | 513 | 0.84 | 1.04 |
| Lumban Julu | 211.36 | 120.82 | 4 | 198 | 647 | 0.66 | 0.22 |
| Silaen | 145.23 | 87.18 | 2 | 128 | 461 | 0.78 | 0.22 |
| Sidamanik | 239.49 | 122.74 | 6 | 222 | 840 | 1.06 | 1.94 |
| Parlilitan | 336.26 | 173.68 | 14 | 312 | 900 | 0.65 | 0.14 |
| Sitinjo | 210.71 | 105.88 | 17 | 200 | 584 | 0.51 | -0.01 |
| Gabe Hutaraja | 175.58 | 102.50 | 2 | 162 | 464 | 0.50 | -0.26 |

To further characterize the rainfall patterns across the Toba Lake region, Table 2 presents a statistical summary of monthly rainfall data from 1981 to 2014 for each observation station. The results reveal substantial spatial heterogeneity in rainfall behavior, with stations such as Parlilitan, Sidamanik, and Merek recording the highest mean rainfall values, large standard deviations, and extreme maximum values that exceed 800 mm. These characteristics are indicative of pronounced inter-annual variability and distributional asymmetry. Most stations exhibit strong positive skewness and heavy right tails, particularly at Merek, Sidamanik, and Laguboti, reflecting asymmetric rainfall distributions. In addition, several stations show substantial excess kurtosis, such as Merek and Dolok Sanggul, suggesting a heightened probability of extreme rainfall events. The standard deviations are also notably large relative to the mean at stations like Parlilitan and Lumban Julu, further underscoring the variability in monthly totals. These statistical features collectively emphasize the inadequacy of traditional symmetric models and underscore the need for more flexible probability distributions that can accommodate skewness, heavy tails, and high variability when modeling rainfall in this hydrologically complex region.

### 3.2.2. Fitted distribution

The APTXL distribution will be fitted to the monthly rainfall data of all 13 stations, using the 34-year period from January 1981 to December 2014. Parameter estimation will be carried out using the maximum likelihood estimation (MLE) method, which provides statistically consistent estimates under regular conditions. To evaluate the performance of the APTXL distribution, it will be compared against several well-established distributions, such as the Gamma, Lognormal, and Generalized Extreme Value (GEV) distributions.

Figure 2 shows the statistical advantages of the APTXL distribution in representing the empirical characteristics of rainfall data. It highlights the ability of the APTXL model to accommodate positive skewness and heavy tails, features commonly observed in tropical rainfall regimes. The comparative density curves show that while classical models provide reasonable fits in moderate ranges, they often underestimate or fail to capture extreme events and sharp peaks. The close alignment of the APTXL distribution with empirical data reinforces its suitability for modeling rainfall phenomena with complex distributional properties, thereby providing a more accurate probabilistic framework for hydrological and climate-related risk analysis.

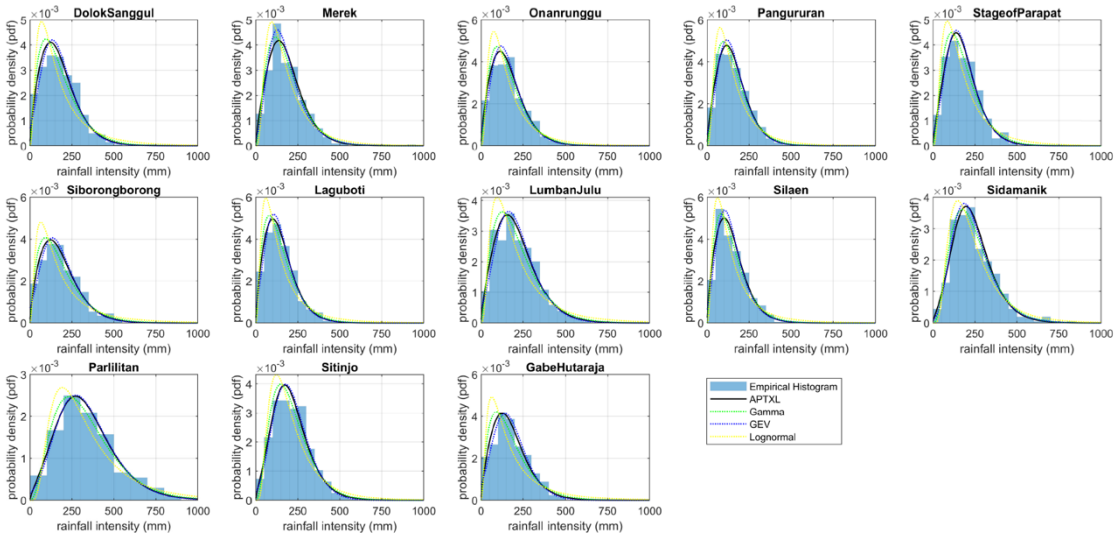


**Figure 2.** Comparison of fitted probability density functions (PDFs) of monthly rainfall data at selected stations using the APTXL, Gamma, Lognormal, and GEV distributions.

Beyond the overall visual fit, Figure 2 also reveals important station-specific insights. At locations such as Merek and Sidamanik, where the empirical histograms exhibit strong right skewness and high variability, the APTXL distribution clearly tracks the upper tail more closely than the Gamma or Lognormal models. In contrast, the GEV distribution occasionally follows the empirical tail but tends to deviate around the central body of the data, indicating a trade-off between fitting extremes and representing average behavior. The robustness of APTXL across diverse stations—including those with moderate rainfall regimes like Pangururan and those with highly variable regimes like Parlilitan—illustrates its adaptability to heterogeneous hydrological conditions. This consistency underscores the practical value of the distribution in multi-station analyses, where a single model must adequately capture a broad spectrum of rainfall characteristics without sacrificing accuracy in either the center or the tails of the distribution.

Table 3 presents a comparative evaluation of four probability distributions applied to monthly rainfall data at selected stations in the Toba Lake region, such as Dolok Sanggul, Merek, and Onanrunggu. To enhance interpretability, each metric value is accompanied by its corresponding rank in parentheses, with rank 1 indicating the best performance among the four models. The results indicate that the APTXL distribution consistently achieves top rankings across multiple criteria and stations. At all three stations, APTXL ranks first in AIC, KS, and CM, and either first or second in RMSE. These results reflect its superior ability to capture both central and tail behaviors in rainfall distributions. In contrast, although classical distributions such as Gamma, Lognormal, and GEV are widely used in hydrological modeling [54], [55], their performance is highly variable across stations. The Lognormal distribution performs poorly across all criteria, consistently receiving the lowest ranks. While Gamma and GEV occasionally show competitive results, particularly in RMSE and KS.

**Table 3.** Comparison of distribution fitting criteria and rankings (in parentheses) for monthly rainfall at Dolok Sanggul, Merek, and Onanrunggu stations.

| Station | Distribution | AIC | RMSE | KS | CM |
|---|---|---|---|---|---|
| Dolok Sanggul | APTXL | **4910.2**$^{(1)}$ | **0.0187**$^{(2)}$ | **0.0417**$^{(1)}$ | **0.1505**$^{(1)}$ |
| | Gamma | 4926.6$^{(4)}$ | 0.0339$^{(3)}$ | 0.0617$^{(3)}$ | 0.4725$^{(3)}$ |
| | GEV | 4924.8$^{(3)}$ | **0.0178**$^{(1)}$ | 0.0480$^{(2)}$ | 0.1646$^{(2)}$ |
| | Lognormal | 4924.0$^{(2)}$ | 0.0627$^{(4)}$ | 0.0886$^{(4)}$ | 1.0181$^{(4)}$ |
| Merek | APTXL | **4875.1**$^{(1)}$ | **0.0167**$^{(1)}$ | **0.0314**$^{(1)}$ | **0.1073**$^{(1)}$ |
| | Gamma | 4908.1$^{(4)}$ | 0.0172$^{(2)}$ | 0.0447$^{(3)}$ | 0.1707$^{(3)}$ |
| | GEV | 4894.4$^{(3)}$ | 0.0180$^{(3)}$ | 0.0338$^{(2)}$ | 0.1370$^{(2)}$ |
| | Lognormal | 4883.5$^{(2)}$ | 0.1210$^{(4)}$ | 0.3052$^{(4)}$ | 1.4057$^{(4)}$ |
| Onanrunggu | APTXL | **4821.8**$^{(1)}$ | **0.0188**$^{(2)}$ | **0.0295**$^{(1)}$ | **0.1208**$^{(1)}$ |
| | Gamma | 4826.7$^{(3)}$ | 0.0272$^{(3)}$ | 0.0400$^{(3)}$ | 0.1986$^{(3)}$ |
| | GEV | 4823.8$^{(2)}$ | **0.0112**$^{(1)}$ | 0.0355$^{(2)}$ | 0.1467$^{(2)}$ |
| | Lognormal | 4882.7$^{(4)}$ | 0.1291$^{(4)}$ | 0.2367$^{(4)}$ | 1.2568$^{(4)}$ |

To synthesize the results across all stations and metrics, the distributions were ranked using the Comprehensive Rating Index (CRI), which aggregates performance across multiple criteria. To illustrate how the Comprehensive Rating Index was derived, consider the rainfall data from Dolok Sanggul station. For this station, each of the four candidate distributions—APTXL, Gamma, GEV, and Lognormal—was evaluated under four statistical criteria: AIC, RMSE, KS, and CM. For every criterion, the models were ranked from best (rank 1) to worst (rank 4), with lower values indicating superior performance. At Dolok Sanggul, the APTXL distribution obtained rank 1 for AIC, rank 2 for RMSE, rank 1 for KS, and rank 1 for CM. Summing these values gives a total score of five. By contrast, the Gamma distribution scored much higher, with ranks of four, three, three, and three, for a total of thirteen, while the Lognormal distribution accumulated the worst score of fourteen. The GEV distribution occupied an intermediate position with a total score of nine. Once ranks have been assigned for each metric and station, they are aggregated across all thirteen stations and all four criteria, producing a cumulative rank sum for every distribution. The CRI value is then calculated by normalizing this sum against the maximum and minimum possible rank totals, thereby ensuring comparability across stations and metrics. A distribution with consistently good performance will achieve a low aggregate rank sum and thus a higher CRI value. For Dolok Sanggul alone, the partial comparison already reveals the advantage of the APTXL distribution, and when the scores from all stations are combined, APTXL emerges as the overall best performer with the highest CRI value, confirming its superior ability to represent rainfall data across diverse conditions. Table 4 summarizes the total rank scores, CRI values, and overall rankings for each distribution across all stations and metrics.

**Table 4.** Summary of distribution performance based on total rank and Comprehensive Rating Index (CRI) across all stations and metrics.

| Distribution | Sum Rank | CRI | Ranking |
|---|---|---|---|
| APTXL | 62 | 0.7019 | 1st |
| GEV | 120 | 0.4231 | 2nd |
| Gamma | 137 | 0.3413 | 3rd |
| Lognormal | 192 | 0.0769 | 4th |

The results demonstrate that the APTXL distribution is the most consistent and superior performer, achieving the highest CRI value and the lowest total rank. This confirms the earlier station-level findings, where APTXL often ranked first or second across all four-evaluation metrics. The GEV distribution ranks second overall, indicating relatively good but less consistent performance. The Gamma distribution ranks third, while the Lognormal distribution ranks last, with a CRI close to zero, highlighting its poor adaptability to the rainfall data in this study.

Overall, these findings validate the effectiveness of the APTXL distribution as a robust probabilistic model for representing monthly rainfall patterns in the Toba Lake region. Its ability to consistently outperform established models across diverse metrics and locations makes it a strong candidate for future hydrological modeling and climate-related applications.

## 4. CONCLUSION

This study introduced and evaluated the Alpha Power Transformed X-Lindley (APTXL) distribution as a flexible probability model for representing monthly rainfall in the Toba Lake region. By incorporating an additional shape parameter through the alpha power transformation, APTXL was able to capture the pronounced skewness, heavy tails, and variability that characterize tropical rainfall data. Comparative analysis against the Gamma, Lognormal, and Generalized Extreme Value (GEV) distributions demonstrated that APTXL consistently achieved superior performance across multiple goodness-of-fit criteria, a result further supported by the Comprehensive Rating Index. Based on these findings, the APTXL distribution is recommended in practice as a robust alternative for hydrological and climatological applications where accurate characterization of extremes is essential, such as flood risk management, reservoir operation, and agricultural water allocation.

Despite its strong performance, the present analysis is subject to several limitations. The model fitting assumed temporal independence of monthly rainfall series and stationarity of the underlying distribution over the 34-year period. These assumptions simplify estimation but may not hold under real climate variability and long-term climate change, where autocorrelation and shifting rainfall regimes are expected. Furthermore, the evaluation relied on maximum likelihood estimation under the frequentist framework, which does not explicitly quantify parameter uncertainty beyond asymptotic properties.

Future research could address these limitations in several ways. Bayesian estimation techniques would provide a natural framework for incorporating prior knowledge and quantifying full parameter uncertainty. Regionalization approaches that pool information across neighboring stations could improve stability of parameter estimates in data-scarce areas, while explicitly accounting for spatial dependence. Finally, extending the APTXL distribution to non-stationary settings—where parameters evolve over time in response to climate drivers—would broaden its applicability to climate change impact studies and long-term water-resource planning.

**ACKNOWLEDGEMENTS**

The authors would like to express their sincere gratitude to all individuals and institutions who contributed to the successful completion of this research. Special thanks are extended to the School of Data Science, Mathematics, and Informatics, IPB University, as well as the Research Center for Climate and Atmosphere, National Research and Innovation Agency (BRIN), for their support and collaboration. This research was financially supported by IPB University through the "Dana Masyarakat IPB Tahun Anggaran 2025", under the "Skema Penelitian Dosen Muda Tahun Anggaran 2025", with Grant Number 10816/IT3.D10/PT.01.03/P/B/2025. The support is gratefully acknowledged. This research was financially supported by IPB University through the Dana Masyarakat IPB Tahun Anggaran 2025, under the Skema Penelitian Dosen Muda Tahun Anggaran 2025, with Grant Number 10816/IT3.D10/PT.01.03/P/B/2025.

## 5. REFERENCES


[1] E. Deal, J. Braun, and G. Botter, "Understanding the Role of Rainfall and Hydrology in Determining Fluvial Erosion Efficiency," Journal of Geophysical Research: Earth Surface, vol. 123, no. 4, pp. 744–778, 2018, doi: 10.1002/2017JF004393.

[2] Z. Sokol, J. Szturc, J. Orellana-Alvear, J. Popová, A. Jurczyk, and R. Célleri, "The role of weather radar in rainfall estimation and its application in meteorological and hydrological modelling —A review," Remote Sensing, vol. 13, no. 3, pp. 1–38, 2021, doi: 10.3390/rs13030351.

[3] M. Dumont et al., "Assessing rainfall global products reliability for water resource management in a tropical volcanic mountainous catchment," Journal of Hydrology: Regional Studies, vol. 40, p. 101037, 2022, doi: 10.1016/j.ejrh.2022.101037.

[4] E. Bessah, E. A. Boakye, S. K. Agodzo, E. Nyadzi, I. Larbi, and A. Awotwi, "Increased seasonal rainfall in the twenty-first century over Ghana and its potential implications for agriculture productivity," Environment, Development and Sustainability, vol. 23, no. 8, pp. 12342–12365, 2021, doi: 10.1007/s10668-020-01171-5.

[5] S. Benziane, "Survey: Rainfall Prediction Precipitation, Review of Statistical Methods," WSEAS Transactions on Systems, vol. 23, pp. 47–59, 2024, doi: 10.37394/23202.2024.23.5.

[6] J. A. Marengo, P. I. Camarinha, L. M. Alves, F. Diniz, and R. A. Betts, "Extreme Rainfall and Hydro-Geo-Meteorological Disaster Risk in 1.5, 2.0, and 4.0°C Global Warming Scenarios: An Analysis for Brazil," Frontiers in Climate, vol. 3, p. 610433, 2021, doi: 10.3389/fclim.2021.610433.

[7] E. Bevacqua, G. Zappa, F. Lehner, and J. Zscheischler, "Precipitation trends determine future occurrences of compound hot–dry events," Nature Climate Change, vol. 12, no. 4, pp. 350–355, 2022, doi: 10.1038/s41558-022-01309-5.

[8] L. Gimeno et al., "Extreme precipitation events," Wiley Interdisciplinary Reviews: Water, vol. 9, no. 6, p. e1611, 2022, doi: 10.1002/wat2.1611.

[9] R. Satyaningsih, V. Jetten, J. Ettema, A. Sopaheluwakan, L. Lombardo, and D. E. Nuryanto, "Dynamic rainfall thresholds for landslide early warning in Progo Catchment, Java, Indonesia," Natural Hazards, vol. 119, no. 3, pp. 2133–2158, 2023, doi: 10.1007/s11069-023-06208-2.

[10] E. Yanfatriani et al., "Extreme Rainfall Trends and Hydrometeorological Disasters in Tropical Regions: Implications for Climate Resilience," Emerging Science Journal, vol. 8, no. 5, pp. 1860–1874, 2024, doi: 10.28991/ESJ-2024-08-05-012.

[11] C. A. Chesner, "The Toba Caldera Complex," Quaternary International, vol. 258, pp. 5–18, 2012, doi: 10.1016/j.quaint.2011.09.025.

[12] H. Irwandi, M. S. Rosid, and T. Mart, "The effects of ENSO, climate change and human activities on the water level of Lake Toba, Indonesia: a critical literature review," Geoscience Letters, vol. 8, no. 1, p. 21, 2021, doi: 10.1186/s40562-021-00191-x.

[13] E. Cristiano, M. C. Ten Veldhuis, and N. Van De Giesen, "Spatial and temporal variability of rainfall and their effects on hydrological response in urban areas - A review," Hydrology and Earth System Sciences, vol. 21, no. 7, pp. 3859–3878, 2017, doi: 10.5194/hess-21-3859-2017.

[14] T. Meema, Y. Tachikawa, Y. Ichikawa, and K. Yorozu, "Real-time optimization of a large-scale reservoir operation in Thailand using adaptive inflow prediction with medium-range ensemble precipitation forecasts," Journal of Hydrology: Regional Studies, vol. 38, 2021, doi: 10.1016/j.ejrh.2021.100939.

[15] V. Anupoju, B. P. Kambhammettu, and S. K. Regonda, "Role of Short-Term Weather Forecast Horizon in Irrigation Scheduling and Crop Water Productivity of Rice," Journal of Water Resources Planning and Management, vol. 147, no. 8, 2021, doi: 10.1061/(asce)wr.1943-5452.0001406.

[16] Y. Zhang and J. M. Swaminathan, "Improved crop productivity through optimized planting schedules," Manufacturing and Service Operations Management, vol. 22, no. 6, pp. 1165–1180, 2020, doi: 10.1287/MSOM.2020.0941.

[17] I. G. Prihanto et al., "A technology acceptance model of satellite-based hydrometeorological hazards early warning system in Indonesia: an-extended technology acceptance model," Cogent Business and Management, vol. 11, no. 1, 2024, doi: 10.1080/23311975.2024.2374880.

[18] A. Susandi et al., "Development of hydro-meteorological hazard early warning system in Indonesia," Journal of Engineering and Technological Sciences, vol. 50, no. 4, pp. 461–478, 2018, doi: 10.5614/j.eng.technol.sci.2018.50.4.2.

[19] L. Alfieri and J. Thielen, "A European precipitation index for extreme rain-storm and flash flood early warning," Meteorological Applications, vol. 22, no. 1, pp. 3–13, 2015, doi: 10.1002/met.1328.

[20] W. Yuan et al., "Study on the Early Warning for Flash Flood Based on Random Rainfall Pattern," Water Resources Management, vol. 36, no. 5, pp. 1587–1609, 2022, doi: 10.1007/s11269-022-03106-3.

[21] D. Li, Z. Liu, D. Wang, and X. Liu, "Rainfall temporal variability-oriented optimization of urban water resources allocation," Journal of Hydrology: Regional Studies, vol. 61, 2025, doi: 10.1016/j.ejrh.2025.102694.

[22] M. Ali, R. C. Deo, Y. Xiang, Y. Li, and Z. M. Yaseen, "Forecasting long-term precipitation for water resource management: a new multi-step data-intelligent modelling approach," Hydrological Sciences Journal, vol. 65, no. 16, pp. 2693–2708, 2020, doi: 10.1080/02626667.2020.1808219.

[23] P. de S. M. P. Ximenes, A. S. Alves da Silva, F. Ashkar, and T. Stosic, "Best-fit probability distribution models for monthly rainfall of Northeastern Brazil," Water Science and Technology, vol. 84, no. 6, pp. 1541–1556, 2021, doi: 10.2166/wst.2021.304.
[24] N. F. E. M. Johar, A. Senawi, and N. A. A. A. Ghani, "An assessment of rainfall distribution in Kuantan river basin using generalized extreme value distribution and Gamma distribution," in AIP Conference Proceedings, 2024. doi: 10.1063/5.0192286.
[25] G. Arriola, L. Villegas, J. Fernandez, J. Vallejos, and C. Idrogo, "Assessment of Parameters of the Generalized Extreme Value Distribution in Rainfall of the Peruvian North," Revista Politecnica, vol. 52, no. 2, pp. 99–112, 2023, doi: 10.33333/rp.vol52n2.10.
[26] B. Moccia, C. Mineo, E. Ridolfi, F. Russo, and F. Napolitano, "Probability distributions of daily rainfall extremes in Lazio and Sicily, Italy, and design rainfall inferences," Journal of Hydrology: Regional Studies, vol. 33, p. 100771, 2021, doi: 10.1016/j.ejrh.2020.100771.
[27] Y. Hundecha, M. Pahlow, and A. Schumann, "Modeling of daily precipitation at multiple locations using a mixture of distributions to characterize the extremes," Water Resources Research, vol. 45, no. 12, 2009, doi: 10.1029/2008WR007453.
[28] J. Y. Shin, T. Lee, and T. B. M. J. Ouarda, "Heterogeneous mixture distributions for modeling multisource extreme rainfalls," Journal of Hydrometeorology, vol. 16, no. 6, pp. 2639–2657, 2015, doi: 10.1175/JHM-D-14-0130.1.
[29] M. K. Najib, S. Nurdiati, and A. Sopaheluwakan, "Copula-based joint distribution analysis of the ENSO effect on the drought indicators over Borneo fire-prone areas," Modeling Earth Systems and Environment, vol. 8, no. 2, pp. 2817–2826, 2022, doi: 10.1007/s40808-021-01267-5.
[30] S. Liu and X. Dong, "The return period analysis of heavy rainfall disasters based on copula joint statistical modeling," Geomatics, Natural Hazards and Risk, vol. 16, no. 1, 2025, doi: 10.1080/19475705.2025.2483799.
[31] N. Alsadat, "A new extension of XLindley distribution with mathematical properties, estimation, and application on the rainfall data," Heliyon, vol. 10, no. 19, 2024, doi: 10.1016/j.heliyon.2024.e38143.
[32] S. Dey, I. Ghosh, and D. Kumar, "Alpha-Power Transformed Lindley Distribution: Properties and Associated Inference with Application to Earthquake Data," Annals of Data Science, vol. 6, no. 4, pp. 623–650, 2019, doi: 10.1007/s40745-018-0163-2.
[33] S. J. Dugasa, A. T. Goshu, and B. G. Arero, "Alpha Power Transformation of the Lindley Probability Distribution," Journal of Probability and Statistics, vol. 2024, no. 1, 2024, doi: 10.1155/2024/9068114.
[34] F. Y. Eissa and C. D. Sonar, "Alpha Power Transformed Extended power Lindley Distribution," Journal of Statistical Theory and Applications, vol. 22, no. 1–2, pp. 1–18, 2023, doi: 10.1007/s44199-022-00051-3.
[35] A. M. Gemeay et al., "The power new XLindley distribution: Statistical inference, fuzzy reliability, and applications," Heliyon, vol. 10, no. 17, 2024, doi: 10.1016/j.heliyon.2024.e36594.
[36] P. J. Northrop, "Stochastic Models of Rainfall," Annual Review of Statistics and Its Application, vol. 11, no. 1, pp. 51–74, 2024, doi: 10.1146/annurev-statistics-040622-023838.
[37] M. F. R. Gaona, K. Michaelides, and M. B. Singer, "STORM v.2: A simple, stochastic rainfall model for exploring the impacts of climate and climate change at and near the land surface in gauged watersheds," Geoscientific Model Development, vol. 17, no. 13, pp. 5387–5412, 2024, doi: 10.5194/gmd-17-5387-2024.
[38] T. Rasool, S. Sahoo, R. Das Bhowmik, and D. Nagesh Kumar, "Development of a stochastic rainfall generator to yield unprecedented rainfall events," Journal of Hydrology, vol. 641, 2024, doi: 10.1016/j.jhydrol.2024.131809.
[39] R. Montes-Pajuelo, Á. M. Rodríguez-Pérez, R. López, and C. A. Rodríguez, "Analysis of Probability Distributions for Modelling Extreme Rainfall Events and Detecting Climate Change: Insights from Mathematical and Statistical Methods," Mathematics, vol. 12, no. 7, 2024, doi: 10.3390/math12071093.
[40] R. L. T. Henriksen, J. B. Hubrechts, J. K. Møller, P. Knudsen, and J. W. Pedersen, "Large-scale rain gauge network optimization using a kriging emulator," Journal of Hydrology, vol. 637, 2024, doi: 10.1016/j.jhydrol.2024.131360.
[41] S. M. Tabatabaei, M. Dastourani, S. Eslamian, and M. Nazeri Tahroudi, "Ranking and optimizing the rain-gauge networks using the entropy–copula approach (Case study of the Siminehrood Basin, Iran)," Applied Water Science, vol. 12, no. 9, 2022, doi: 10.1007/s13201-022-01735-y.
[42] A. H. Hussein and M. N. Kasim, "Utilizing statistical distribution tests to develop rainfall intensity–duration–frequency curves for enhanced hydrological analysis in Kirkuk city, Iraq," Water Practice and Technology, vol. 19, no. 11, pp. 4378–4389, 2024, doi: 10.2166/wpt.2024.258.
[43] A. Mahdavi and D. Kundu, "A new method for generating distributions with an application to exponential distribution," Communications in Statistics - Theory and Methods, vol. 46, no. 13, pp. 6543–6557, 2017, doi: 10.1080/03610926.2015.1130839.
[44] M. Nassar, A. Alzaatreh, M. Mead, and O. Abo-Kasem, "Alpha power Weibull distribution: Properties and applications," Communications in Statistics - Theory and Methods, vol. 46, no. 20, pp. 10236–10252, 2017, doi: 10.1080/03610926.2016.1231816.
[45] A. M. Basheer, "Alpha power inverse Weibull distribution with reliability application," Journal of Taibah

University for Science, vol. 13, no. 1, pp. 423–432, 2019, doi: 10.1080/16583655.2019.1588488.
[46] S. Dey, M. Nassar, and D. Kumar, "Alpha power transformed inverse Lindley distribution: A distribution with an upside-down bathtub-shaped hazard function," Journal of Computational and Applied Mathematics, vol. 348, pp. 130–145, 2019, doi: 10.1016/j.cam.2018.03.037.
[47] S. Ihtisham, A. Khalil, S. Manzoor, S. A. Khan, and A. Ali, "Alpha-Power Pareto distribution: its properties and applications," PLoS ONE, vol. 14, p. e0218027, 2019.
[48] R. A. Zeineldin, M. Ahsan Ul Haq, S. Hashmi, and M. Elsehety, "Alpha Power Transformed Inverse Lomax Distribution with Different Methods of Estimation and Applications," Complexity, vol. 2020, pp. 1–15, 2020, doi: 10.1155/2020/1860813.
[49] S. Chouia and H. Zeghdoudi, "The X-Lindley distribution: properties and application," Journal of Statistical Theory and Applications, vol. 20, no. 2, pp. 318–327, 2021.
[50] J. C. Lagarias, J. A. Reeds, M. H. Wright, and P. E. Wright, "Convergence properties of the Nelder-Mead simplex method in low dimensions," SIAM Journal on Optimization, vol. 9, no. 1, pp. 112–147, 1998, doi: 10.1137/S1052623496303470.
[51] M. A. Baig et al., "Evaluation and Projection of Temperatures Over Pakistan: Insights from the Downscaled NEX-GDDP-CMIP6 Models," Earth Systems and Environment, 2025, doi: 10.1007/s41748-024-00554-2.
[52] Z. Jiang, W. Li, J. Xu, and L. Li, "Extreme precipitation indices over China in CMIP5 models. Part I: Model evaluation," Journal of Climate, vol. 28, no. 21, pp. 8603–8619, 2015, doi: 10.1175/JCLI-D-15-0099.1.
[53] L. D. Ribeiro-Reis, "The kagebushin-beta distribution: an alternative for gamma, Weibull and exponentiated exponential distributions," Journal of the Egyptian Mathematical Society, vol. 30, no. 1, 2022, doi: 10.1186/s42787-022-00158-7.
[54] M. Farooq, M. Shafique, and M. S. Khattak, "Flood frequency analysis of river swat using Log Pearson type 3, Generalized Extreme Value, Normal, and Gumbel Max distribution methods," Arabian Journal of Geosciences, vol. 11, no. 9, 2018, doi: 10.1007/s12517-018-3553-z.
[55] W. Szulczewski and W. Jakubowski, "The Application of Mixture Distribution for the Estimation of Extreme Floods in Controlled Catchment Basins," Water Resources Management, vol. 32, no. 10, pp. 3519–3534, 2018, doi: 10.1007/s11269-018-2005-6.